# Journal of Applied Sciences

ISSN 1812-5654

science alert

ANSInet
an open access publisher
http://ansinet.com

Journal of Applied Sciences 8 (19): 3431-3438, 2008
ISSN 1812-5654


# Automatic Main Road Extraction from High Resolution Satellite Imageries by Means of Self-Learning Fuzzy-GA Algorithm

[1]A. Mohammadzadeh, [1]M.J. Valadan Zoej and [2]A. Tavakoli
[1]Department of Remote Sensing, K.N. Toosi University of Technology, Tehran, Iran
[2]Department of Electrical Engineering, Amirkabir University, Tehran, Iran

**Abstract:** In this study, using few samples from road surface, a continuous genetic algorithm is applied to a fuzzy based mean calculation system to obtain road mean values in each band of high resolution satellite colour images. Then, the images are segmented using the calculated mean values from the self-learning fuzzy-GA system. The proposed self-learning fuzzy-GA algorithm calculated best mean value with sub grey level precision. The method is applied to simulated images where the calculated mean values are consistent with the hypothetic mean values. Application of the method to IKONOS satellite images has shown a prospective outcome. Mathematical morphology is subsequently used to extract an initial main road centerline from the segmented image. Then, small redundant segments are automatically removed. The quality of the extracted road centerline indicates the effectiveness of the proposed approach.

**Key words:** Fuzzy logic, road centerline extraction, continuous genetic algorithm, mathematical morphology, IKONOS, image segmentation

## INTRODUCTION

Nowadays, many organizations have growing demands for fast, accurate and cost effective geospatial information specially roads from satellite and aerial images. The traditional manual extraction of road is expensive and time consuming. Alternatively, to overcome the mentioned deficiencies, automatic extraction algorithms would reduce human interactions in the road extraction. This will reduce the cost considerably and will be time saving. In automatic extraction of roads, Mena (2003) has made a review of over 250 references in road extraction. Also Mena and Malpica (2005), Baltsavias (2004) and Quackenbush (2004) have reviewed and analyzed some of the approaches. An efficient automatic extraction algorithm tries to simulate human thinking way using some experts' knowledge. Recently, artificial intelligence has become a very efficient tool in human thinking simulation and especially in automatic feature extraction issues (Agouris *et al*., 1998; Mohammadzadeh *et al*., 2006; Mokhtarzade and Valadan Zoej, 2007; Mokhtarzade *et al*., 2007; Amini *et al*., 2002). Artificial intelligence can be built using advanced mathematical theories such as fuzzy logic, artificial neural networks and genetic algorithms. Agouris *et al*. (1998) used fuzzy logic for segmentation of an image. In this method, pixels that are brighter are likely to be closer to real road pixels. Then template matching algorithm is applied along the user defined direction to locate the best road position. Mokhtarzade and Valadan Zoej (2007) examined texture information to design an appropriate multilayer neural network for road detection purpose. Following, optimized texture parameters using artificial neural networks were proposed by Mokhtarzade *et al*. (2007). Mohammadzadeh *et al*. (2006) applied a fuzzy system to detect road surface using few samples from road surface. There is a serious difficulty to find the optimum values of the proposed membership functions. In this method, a blind and discrete search instead of a global and continuous search is performed to define the parameters of the fuzzy membership function. In addition, it is not practical to test all the possible answers to find the best solution. To overcome the mentioned numerical problem, genetic algorithms, as a well-known search and optimization method, have been adapted to adjust parameters of the fuzzy system.

Thus, in this research a self-learning fuzzy-GA system is proposed which the fuzzy system performs reasoning based on a number of fuzzy rules simulating human expert knowledge and meantime genetic algorithm

**Corresponding Author:** Ali Mohammadzadeh, Department of Remote Sensing, Faculty of Surveying, Khaje Nasir Toosi University of Technology, No. 1346, Vali_Asr St., Mirdamad Cr., Postal Code 1996715433, Tehran, Iran Tel: +98 09124752961 Fax: +98 021 88786213

refines parameters of the fuzzy system. Using the proposed new algorithm, the best mean values are determined with sub grey level accuracy. Subsequently, an algorithm based on mathematical morphology is developed to extract road centerline from binary segmented road and non-road image. Finally, the proposed method is applied to a simulated image and high resolution multispectral IKONOS images with very satisfactory results and the comparison has been made to prove its efficiency.

## MATERIALS AND METHODS

In this research, a self-learning fuzzy-GA algorithm is developed to detect road surface from pan-sharpened IKONOS high resolution satellite image. The proposed method utilizes artificial intelligence to achieve more sophisticated and efficient feature extraction algorithms. Significant improvements are presented that increase automation degree, perform global search, high accuracy of 0.5 grey levels for the calculated mean value. Here, a continuous directional search from an initial value towards the final solution in global search space is suggested. These improvements are achieved by applying a continuous genetic algorithm to a fuzzy method. At first, a brief overview is given to the fuzzy cost function. Then the proposed self-learning fuzzy-GA system is described to segment the image into road and non-road. Afterwards, an algorithm based on mathematical morphology is designed to extract road centerline.

**Fuzzy cost function:** For a pixel $X = [x_1, x_2, x_3]^T$ in band b, the well-known Gaussian membership function for a fuzzy linguistic variable in band b can be determined by two parameters: mean value ($M_b$) and standard deviation value ($sigma_b$) as:

$$\text{Gaussian\_Function} = \exp\left(-\frac{(x_b - M_b)^2}{2\,\text{sigma}_b^2}\right) \quad ;b = 1,2,3 \qquad (1)$$

As presented in Mohammadzadeh *et al.* (2006) with some added modifications, considering $mean_b$ as real mean value of road pixels in band (b) and σ as standard deviation of it, five linguistic variables with Gaussian membership functions for each band are defined as:

- Good-Road ($GR_b$)
- Up-Probable-Road ($UPR_b$)
- Down-Probable-Road ($DPR_b$)
- Up-Bad-Road ($UBR_b$)
- Down-Bad-Road ($DBR_b$)

Table 1: Results of mean and SD of the Mfs

| Mfs | Mean value (Grey level) | SD value (Grey level) |
|---|---|---|
| Down-Bad-Road$_b$ ($DBR_b$) | Mean$_b$ –3.5σ | σ/2 |
| Down-Probable-Road$_b$ ($DPR_b$) | Mean$_b$ –2.5σ | σ/2 |
| Good-Road$_b$ ($GR_b$) | Mean$_b$ | σ |
| Up-Probable-Road$_b$ ($UPR_b$) | Mean$_b$ +2.5σ | σ/2 |
| Up-Bad-Road$_b$ ($UBR_b$) | Mean$_b$ +3.5σ | σ/2 |

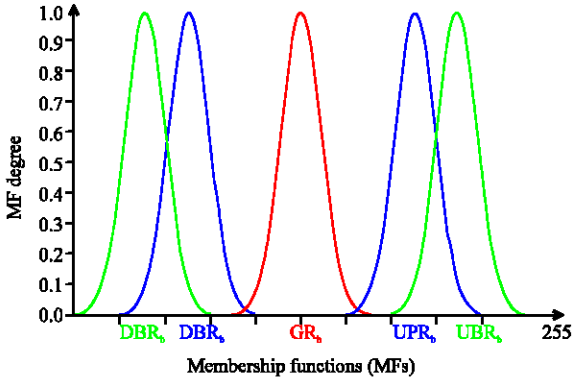


Fig. 1: Position of the membership functions in image band b

The distribution of the above mentioned membership functions and non-road pixels represented by membership function of $DBR_b$ is far from road pixels represented by membership function of $GR_b$ in image band b are shown in Fig. 1.

Linguistic variable of Good-$Road_b$ define the road pixels in image band b. Probable road pixels are identified by linguistic variables of Up-Probable-$Road_b$ or Down-Probable-$Road_b$. Non-road pixels are defined by linguistic variables of Down-bad-$Road_b$ and Up-Bad-$Road_b$. The mean value and standard deviation of the above mentioned membership functions are defined in Table 1. For instance, according to Table 1, membership function of $DBR_b$ has mean value of Mean Value = $mean_b$ –3.5σ and standard deviation of SD = σ/2.

As there are three bands in input image and five fuzzy membership functions in each band, thus, total number of 5×5×5 = 125 classes would be formed by combination of three bands out of the mentioned five membership function and it is shown in Table 2.

By using mean values and SD values of Table 1, all the Gaussian Mfs of Table 2 will be calculated. In Table 2, the Gaussian membership function associated with class c in band b is defined by $f_{b,c}$:

$$f_{b,c} = \exp\left(-\frac{(x_b - \mu_{b,c})^2}{2(\sigma_{b,c})^2}\right) \quad \Rightarrow \quad F = [f_{b,c}]_{3\times 125} \qquad (2)$$

where, $x_b$ is the grey level of any pixel in band b. $\mu_{b,c}$ and $\sigma_{b,c}$ are the mean value and the standard deviation of class c in band b respectively. For example, class c = 1, is

Table 2: Classes of the fuzzy system

| Class | Band 1 | Band 2 | Band 3 |
|---|---|---|---|
| Class C = 1 (non-road) | $f_{1,1}(\mu_{1,1}, \sigma_{1,1}) = DBR_1$ | $f_{1,1}(\mu_{2,1}, \sigma_{2,1}) = DBR_2$ | $f_{3,1}(\mu_{3,1}, \sigma_{3,1}) = DBR_3$ |
| ⋮ (non-road) | | | |
| Class C = 63 (road) | $f_{1,63}(\mu_{1,63}, \sigma_{1,63}) = GR_1$ | $f_{2,63}(\mu_{2,63}, \sigma_{2,63}) = GR_2$ | $f_{3,63}(\mu_{3,63}, \sigma_{3,63}) = GR_3$ |
| Class C = 64 (non-road) | $f_{1,64}(\mu_{1,64}, \sigma_{1,64}) = GR_1$ | $f_{2,64}(\mu_{2,64}, \sigma_{2,64}) = GR_2$ | $f_{3,64}(\mu_{3,64}, \sigma_{3,64}) = UPR_3$ |
| ⋮ (non-road) | | | |
| Class C = 125 (non-road) | $f_{1,125}(\mu_{1,125}, \sigma_{1,125}) = UBR_1$ | $f_{1,125}(\mu_{2,125}, \sigma_{2,125}) = UBR_2$ | $f_{3,125}(\mu_{3,125}, \sigma_{3,125}) = DBR_3$ |

determined by $DBR_1$ in band b = 1, $DBR_2$ in band b = 2 and $DBR_3$ in band b = 3. Therefore according to Table 1 and 2, $\mu_{1,1} = mean_1 - 3.5 \cdot \sigma$ and $\sigma_{1,1} = \frac{\sigma}{2}$ would be obtained for class c = 1 in band b = 1. In this way, all the elements of matrix F for each pixel is generated which is called fuzzification step.

As the next step, fuzzy reasoning procedure consists of finding the maximum among the minimum values of each column and its column number cn defines the class number of the fuzzified pixel. As indicated in Table 2, class number of cn = 63 is road and the rest are non-road. If t is the total number of pixels identifies as road in the fuzzy reasoning step, for a pixel $X_j$ where $1 \le j \le t$:

$$r_j = \begin{bmatrix} r_{1,1} \\ r_{2,1} \\ r_{3,1} \end{bmatrix}_{(X_j)} = \begin{bmatrix} (x_1 - \mu_{1,cn}) \cdot (\frac{1 - f_{1,cn}}{sum(f_{1,1:125})}) \\ (x_2 - \mu_{2,cn}) \cdot (\frac{1 - f_{2,cn}}{sum(f_{2,1:125})}) \\ (x_3 - \mu_{3,cn}) \cdot (\frac{1 - f_{3,cn}}{sum(f_{3,1:125})}) \end{bmatrix}_{(X_j)} \quad (3)$$

$$sig\_cn = \begin{bmatrix} (\sigma_{1,cn})^2 & 0 & 0 \\ 0 & (\sigma_{2,cn})^2 & 0 \\ 0 & 0 & (\sigma_{3,cn})^2 \end{bmatrix} \quad (4)$$

$$c_j = \sqrt{(r_j) \cdot inv(sig\_cn) \cdot (r_j)^T} \Rightarrow sum\_c = \sum_{j=1}^{t} c_j \quad (5)$$

$$d_j = \sum_{b=1}^{3} (1 - \frac{f_{b,cn}}{sum(f_{b,1:125})})^2 \Rightarrow sum\_d = \sum_{j=1}^{t} d_j \quad (6)$$

After applying the procedure to all image pixels, the fuzzy cost function is:

$$Cost(mean_1, mean_2, mean_3; \sigma) = \frac{sum\_c}{sum\_d \cdot t} \quad (7)$$

**Self-learning fuzzy-GA method:** The thought process behind the genetic algorithms (GAs), which are based on genetic processing of biological organisms, are adaptive methods that can be used to solve search and optimization problems. Comparing to traditional optimization algorithms, continuous GA is suitable to optimization problems that use continuous values for the variables (Haupt and Huapt, 2004). Therefore, in this study, a continuous genetic algorithm is used to find optimum parameters of a fuzzy system to obtain best mean value of road with sub pixel accuracy. As shown in Fig. 2, arbitrary user selected pixels of the road define the initial value of the self-learning fuzzy-GA approach. Standard deviation of the road pixel grey level ($\sigma$) is an input to the fuzzy algorithm. By sampling many road surfaces, the standard deviation of 10 are obtained for IKONOS images. It should be noted that even though the homogeneous surface of roads lead to an almost constant standard deviation of $\sigma$ grey level, the calculated mean values are insensitive to unexpected radiometric discrepancies.

As it is shown in Fig. 2, in the proposed self-learning fuzzy-GA method, the fuzzy cost function is fitted to the continuous GA by defining a chromosome as an array of variable values to be optimized. If the chromosome has $N_{var}$ variables (an N-dimensional optimization problem) given by $p_1, p_2, ..., p_{N_{var}}$ then the chromosome is as:

$$Chromosome = [p_1 p_2, ..., p_{N_{var}}] \quad (8)$$

Variable values are represented as floating-point numbers. In this case, each of the chromosomes has three values in the three dimensional search domain that are possible mean values of road in bands 1, 2 and 3. By choosing an arbitrary pixel $Y = [y_1, y_2, ..., y_b, ..., y_B]$ from the road surface, the chromosome has $N_{var} = B$ variables and chromosome maximum and minimum values of chromosome $p_i = [p_{i1}, p_{i2}, ..., p_{ib}, ..., p_{iN_{var}}]$ will be defined as:

$$\forall y_b \in Y, \quad (y_b - 15) \le p_{ib} \le (y_b + 15)] \quad ; b = 1:B \quad (9)$$

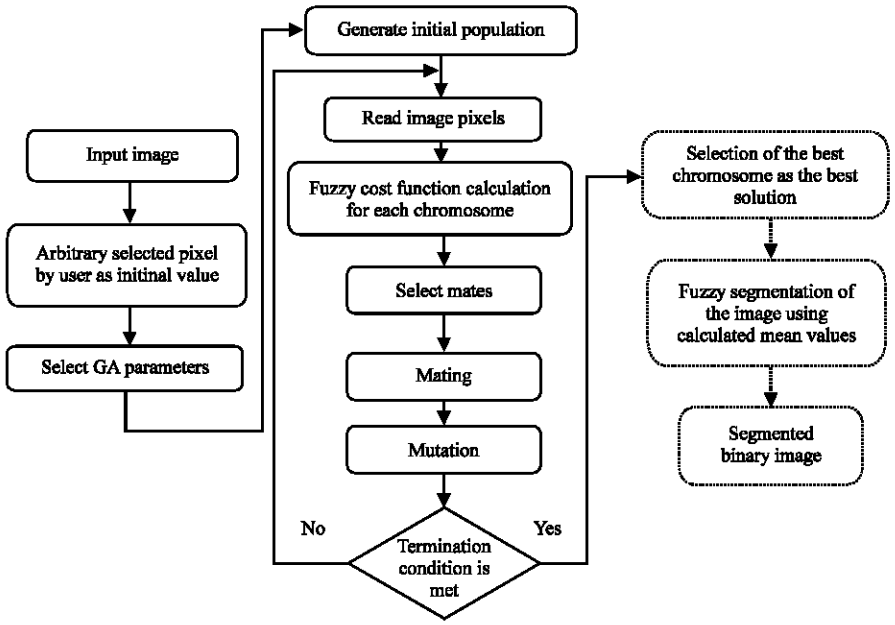


Fig. 2: Block diagram of the self-learning fuzzy-GA process

After defining the parameters of the method, initial population of $N_{pop}$ chromosomes with $N_{var}$ random values, which fall between maximum and minimum values of chromosomes, are generated.

Now is the time to decide which chromosome in the initial population are fit enough to survive and possibly reproduce offspring in the next generation. The $N_{pop}$ costs and associated chromosomes are ranked from lowest point to highest cost and the rest die off. This process of natural selection is must occur in each iteration of the algorithm to allow the population of chromosomes to evolve over the generation to the most fit members as defined by the cost function. Of the $N_{pop}$ chromosomes in a given generation, only the top $N_{keep}$ are kept as parents for mating and the rest are discarded to make room for new offspring.

After selection of the parents, the offspring are generated by some combination of these parents. Huapt and Huapt (2004) presented an efficient mating scheme. It begins by randomly selecting a variable $\alpha$ in the first pair of parents to be the crossover point. mom and dad parents with the crossover point is defined as:

$$\begin{aligned} parents_{mom} &= [p_{m1}, p_{m2}, \cdots p_{m\alpha} \cdots, p_{mN_{var}}] \\ parents_{dad} &= [p_{d1}, p_{d2}, \cdots p_{d\alpha} \cdots, p_{dN_{var}}] \end{aligned} \quad (10)$$

Then the selected variables ($P_{m\alpha}$ and $P_{d\alpha}$) are combined to form the new variables that will appear in the children:

$$\begin{aligned} p_{new1} &= p_{m\alpha} - \beta[p_{m\alpha} - p_{d\alpha}] \\ p_{new2} &= p_{d\alpha} - \beta[p_{m\alpha} - p_{d\alpha}] \end{aligned} \quad (11)$$

where, $\beta$ is a random variable between 0 and 1. Afterwards, the crossover with the rest of the chromosome will complete as:

$$\begin{aligned} offspring_1 &= [p_{m1}, p_{m2}, \cdots p_{new1} \cdots, p_{dN_{var}}] \\ offspring_2 &= [p_{d1}, p_{d2}, \cdots p_{new2} \cdots, p_{mN_{var}}] \end{aligned} \quad (12)$$

To avoid local search, mutation should be done to find the global minimum cost. By choosing a mutation rate, a portion of the chromosomes are selected to be mutated. In fact, a mutated variable is replaced by a new random variable. The described process is iterated until a termination condition is met. For example, if differences of the two consequently calculated best mean values were below a user-defined threshold T then the process will be finished. The last global best position would be considered as the best mean value that is used to calculate the fuzzy matrix $F = [f_{b,c}]_{B\times C}$ where $f_{b,c}$ represent the fuzzy membership degree of class (c) in band (b) for each pixel. Finally, by applying the fuzzy reasoning Min-Max operator, the road and non-road pixels are identified.

**Mathematical morphology:** An algorithm based on mathematical morphology is designed to extract road centerline form the binary image of detected road surface. Traditional pixel based extraction algorithms such as edge

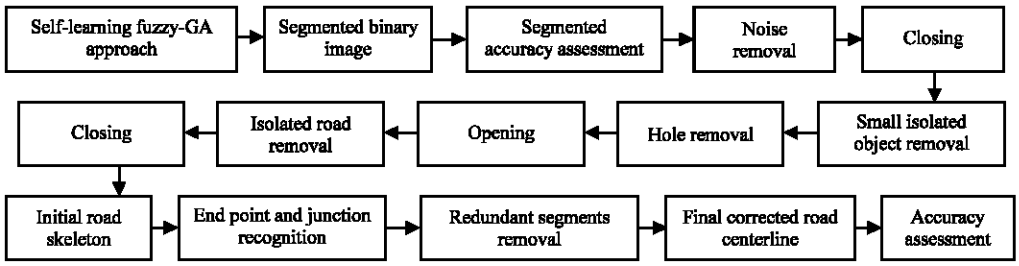


Fig. 3: Flowchart of the road centreline extraction

detection or edge linking do not consider the structure of objects. Therefore, these methods are not suitable enough to extract roads in urban or complex rural areas. On the contrary, morphological operators analyze the image in a manner sensitive to the objects shape (Serra and Vincent, 1992). Therefore, mathematical morphology and mathematical geometry concepts are used to extract road centerline from the segmented binary image (Fig. 3).

As shown in Fig. 3, after applying the proposed self-learning fuzzy-GA method, the input image will be segmented in road and non-road. An accuracy assessment is carried out to assess the efficiency of the self-learning fuzzy-GA segmentation method.

Then, single pixel noise is removed from the binary segmented image. Small gaps are connected by the closing operator. The length of each road segment is obtained by applying morphological pattern spectrum algorithm. Since roads are the longest object in the image, the isolated small objects are distinguished and removed using pattern spectrum algorithm. Radiometric variations on the road such as buildings, trees and shadows create voids on the road surface that are detected and filled. Small narrow paths are removed by an opening operator followed by removal of remaining isolated road objects using pattern spectrum algorithm. Then a closing operator is applied to fill in the gaps produced erroneously by the opening operator. A skeletonization algorithm is applied to extract the initial road centerline. Following that a raster based algorithm is developed and used to detect end points and junctions. Consequently, the smallest line segments that are connected to each junction and are below a threshold level are removed. Through an iterative approach, all auxiliary segments are removed. Finally the extracted road is compared with manually extracted reference map for accuracy assessment of the extraction step.

## RESULTS AND DISCUSSION

**Implementation on simulated image:** A simulated image is produced as reference image to evaluate the accuracy of the proposed self-learning fuzzy-GA approach. Based on values defined in Table 3, four simulated patterns of Fig. 4 are produced. Calculated mean values by self-learning fuzzy-GA method are given in Table 4 which indicates its accuracy and efficiency. The efficiency of the approach is realized by comparing the results of Table 4 with Table 3 where the RMSE is equal to 0.478. Please note, even though the simulated images have a high degree of overlap and various patterns standard deviation, the calculated mean values are still in agreement with the presumed mean values. This indicates the stability of this method even in unprecedented situations.

Table 3: Values used for pattern generation

| | Band 1 (Grey level) | | Band 2 (Grey level) | | Band 3 (Grey level) | |
|---|---|---|---|---|---|---|
| Pattern | $\mu_1$ | $\sigma_1$ | $\mu_2$ | $\sigma_2$ | $\mu_3$ | $\sigma_3$ |
| a | 140.3 | 6 | 93.2 | 9 | 104.8 | 8 |
| b | 82.7 | 7 | 113.7 | 6 | 125.9 | 4 |
| c | 123.3 | 8 | 137.5 | 10 | 86.4 | 7 |
| d | 98.7 | 10 | 158.3 | 9 | 63.1 | 6 |

Table 4: Computed mean values of patterns

| | Self-learning fuzzy-GA method | | |
|---|---|---|---|
| | Band 1 (Grey level) | Band 2 (Grey level) | Band 3 (Grey level) |
| Pattern | $\mu_1$ | $\mu_2$ | $\mu_3$ |
| a | 140.27 | 92.89 | 104.31 |
| b | 82.73 | 112.55 | 125.81 |
| c | 123.86 | 137.14 | 86.82 |
| d | 99.22 | 158.64 | 62.84 |
| RMSE = 0.478 | | | |

**Implementation on high resolution satellite image:** This method is applied on a pan-sharpened IKONOS image of Kish Island in south of Iran that is shown in Fig. 5a. The 8 bit image format of IKONOS has three spectral bands of 1 m ground resolution. Figure 5b shows the manually produced reference map of the same region. The self-learning fuzzy-GA algorithm is applied to segment the image. Geospatial objects such as buildings, cars, shadows, scattered clay on the road, fresh asphalt cover

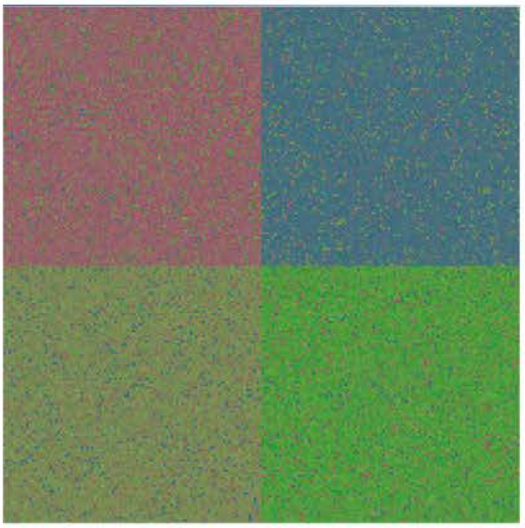

Fig. 4: Final simulated image of patterns (a) to (d)

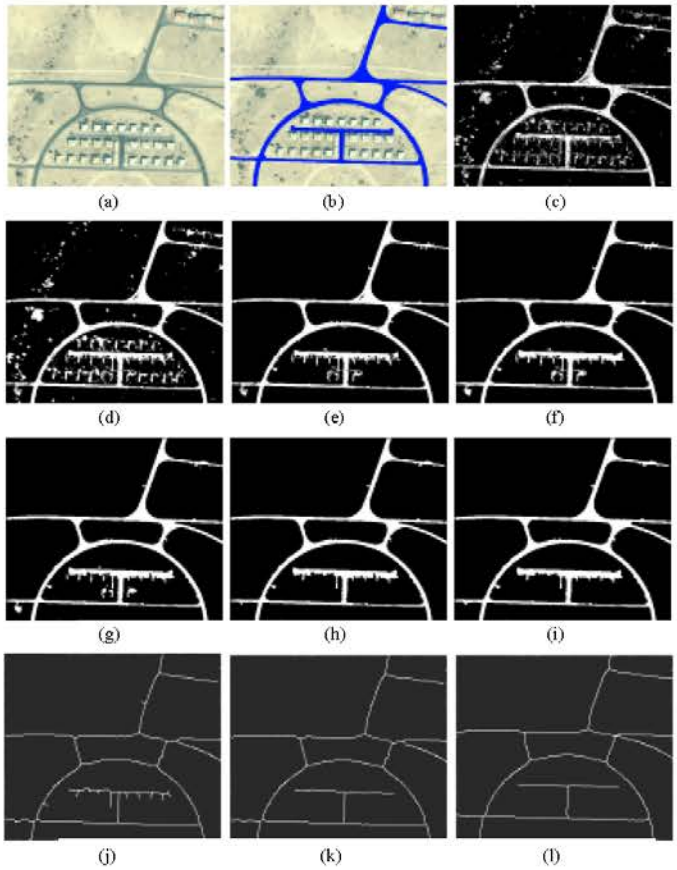


Fig. 5: (a) IKONOS image from Kish Island in Iran, (b) Manually produced reference map, (c) Segmented road pixels by self-learning fuzzy-GA method, (d) Single noise and small gap removal, (e) Small isolated object removal, (f) Hole removal, (g) Opening, (h) Isolated road removal, (i) Closing, (j) Initial extracted road, (k) Small segments removal as final corrected road centreline and (l) Manually produced road skeleton ground truth

Table 5: Image and the parameters used in road extraction procedure

| | | Self-learning fuzzy-GA method | | | | | |
|---|---|---|---|---|---|---|---|
| | | Initial mean value for each subclass (Grey scale) | | | Calculated mean value for each subclass (Grey scale) | | |
| High resolution colour image | Image size (pixel) | Band 1 (Grey level) | Band 2 (Grey level) | Band 3 (Grey level) | Band 1 (Grey level) | Band 2 (Grey level) | Band 3 (Grey level) |
| IKONOS image of | 541×460 | 93 | 122 | 119 | 104.06 | 130.37 | 122.78 |
| Kish Island (Fig. 4) | | 153 | 168 | 153 | 144.36 | 162.22 | 145.52 |

and road pixel radiometric variations complicate the extraction process. In such cases, the detected road by one subclass does not represent the road surface adequately and the user must select a sample from uncovered part to segment remaining discrepancies. Therefore, in this case, two road subclasses exist and one sample from the road surface is used as inputs to the algorithm to detect each road subclass. Traditional classification methods rely on manual sampling to get mean values that are user dependent, but this method uses a single best mean value for each subclass. The implemented GA uses 16 chromosomes ($N_{pop}$) in each population generation. The mutation rate is 0.15 and half of the population is kept for mating. The total number of iterations should not exceed a user defined threshold of $iter_{tr}$ = 15. The calculated best mean values for subclasses of Fig. 5a are summarized in Table 5.

Figure 5c represents the final segmentation result using the values of Table 4. Comparing Fig. 5a and c, we observe that radiometric similarities have resulted in misclassification of objects as road. Misclassified objects that are connected to road create serious difficulties in the road extraction process. Figure 5b and c are compared for accuracy assessment. The road detection correctness coefficient (RCC) is defined as the ratio of the total correctly identified road pixels to the total reference road pixels. Background detection correctness coefficient (BCC) is similarly defined for non-road pixels. Overall accuracy is the percentage of correctly classified pixels to all available pixels in the image and kappa coefficient is a representation of stability of classification. For the IKONOS image of Fig. 5c, RCC of 0.7715, BCC of 0.9621, overall accuracy of 0.9419 and kappa coefficient of 0.7049 are obtained. Figure 5d shows the result of one pixel size noise removal followed by a 3×3 pixel closing operator to fill small holes and gaps. Due to identification of some objects as road, an appropriate image processing operator that is sensitive to the geometry of the objects and also considers the neighbourhood connectivity information is needed for output correction. Traditional pixel based edge-line detection algorithms are not sensitive to the geometry of the objects. On the other hand, binary mathematical morphology operators are structure-based, nonlinear and sensitive to the shape and size of the objects, thus, roads as a narrow and elongated object could be differentiated. It should be noted that in mathematical morphology, an appropriate structuring element architecture, size, type and priority of the morphological operator must be defined. Granulometry operator analyzes all object lengths in the image by applying an opening operator to the image and separating various objects as different images. Then, the resultant images are compared with the input image to find the shape and size signature of each object which is known as pattern spectrum. Pattern spectrum was introduced by Serra and Vincent (1992) enables objects detection without affecting their shape and size. Starting from a point and iterating T times to cover the whole surface of the object, the object length is represented by T. All objects lengths of less than a user defined threshold (e.g., $T_{tr}$ = 70) are omitted as shown in Fig. 5e.

Even though misidentified objects are removed form the image, Fig. 5 indicates that some deficiencies such as large holes continue to remain. Using an algorithm to detect dark areas encompassed by the road, the remaining large holes are removed as shown in Fig. 5f. Narrow paths are removed by applying an opening operator with structure element size of 3×3 pixels as shown in Fig. 5g. Figure 5h depicts the application of a pattern spectrum to remove small isolated objects. In Fig. 5i, a 7×7 pixel closing operator is applied to fill unexpected small gaps produced in Fig. 5h. Initial extracted skeleton of the road is shown in Fig. 5j. First, starting from an end point, the segment is traced to a junction point. Then, if the segment length is smaller than a threshold level (e.g. $T_{tr}$ =15), it is omitted. In Fig. 5k, small segments are detected and removed in an iterative manner. Extracted road centreline of Fig. 5k indicates the effectiveness of the method even in the presence of road disturbing objects and radiometric variations. Comparison of the automatically extracted road centreline of Fig. 5k with the manually pixel-by-pixel produced centreline of Fig. 5l indicates an excellent agreement with a Root Mean Square Error (RMSE) of only 1.0428 pixels.

## CONCLUSION

In this study, the road centreline is extracted from high resolution satellite imagery by applying the genetic algorithm optimization algorithm on a fuzzy based

approach. Working in raster space, an algorithm based on mathematical morphology and geometric concepts is developed to extract a refined road centreline. It is shown that the road is effectively detected and extracted. The accuracy of image segmentation and road centreline extraction is shown by a comparison to manually generated road map and skeleton. The achieved results indicate accuracy and efficiency of the proposed self-learning fuzzy-GA method. In addition, end points, junctions and segments are recognized automatically enabling removal of small redundant segments leading to more reliable extracted road centreline. The automatically extracted skeleton of the road can be readily inserted in a GIS database.

## REFERENCES

Agouris, P., S. Gyftakis and A. Stefanidis, 1998. Using a fuzzy supervisor for object extraction within an integrated geospatial environment. Int. Arch. Photogram. Remote Sens., 32: 191-195.

Amini, J., M.R. Saradjian, J.A.R. Blais, C. Lucas and A. Azizi, 2002. Automatic road-side extraction from large scale image maps. Int. J. Applied Earth Observ. Geoinform., 4: 95-107.

Baltsavias, E.P., 2004. Object extraction and revision by image analysis using existing geodata and knowledge: Current status and steps towards operational systems. ISPRS J. Photogrammetry Remote Sens., 58: 129-151.

Haupt, R.L. and S.E. Haupt, 2004. Practical Genetic Algorithms. 2nd Edn., John Wiley and Sons Ltd., New Jersey, ISBN: 0471671754.

Mena, J.B., 2003. State of the art on automatic road extraction for GIS update: A novel classification. Pattern Recog. Lett., 24: 3037-3058.

Mena, J.B. and J.A. Malpica, 2005. An automatic method for road extraction in rural and semi-urban areas starting from high resolution satellite imagery. Pattern Recognit. Lett., 26: 1201-1220.

Mohammadzadeh, A., A. Tavakoli and M.J. Valadan Zoej, 2006. Road extraction based on fuzzy logic and mathematical morphology from pan-sharpened IKONOS images. The Photogram. Record, 21: 44-60.

Mokhtarzade, M. and M.J. Valadan Zoej, 2007. Road detection from high resolution satellite images using artificial neural networks. Int. J. Applied Earth Observ. Geoinform., 9: 32-40.

Mokhtarzade, M., H. Ebadi and M.J. Valadan Zoej, 2007. Optimization of road detection from high-resolution satellite images using texture parameters in neural network classifiers. Can. J. Remote Sens., 33: 481-491.

Quackenbush, L.J., 2004. A review of techniques for extracting linear features from imagery. Photogram. Eng. Remote Sens., 70: 1383-1392.

Serra, J. and L. Vincent, 1992. An overview of morphological filtering. Circuits Syst. Signal Process., 11: 47-108.